

# Waveguide-Ring Resonator Coupler with Class-F Rectifier for 2-D Waveguide Power Transmission

Akihito Noda and Hiroyuki Shinoda

Department of Information Physics and Computing, The University of Tokyo

7-3-1 Hongo, Bunkyo-ku, Tokyo, 113-8656, Japan

Email: Akihito\_Noda@ipc.i.u-tokyo.ac.jp; shino@alab.t.u-tokyo.ac.jp

**Abstract**—In this paper we demonstrate a high-efficiency dc power extraction using a rectifying coupler in a two-dimensional waveguide power transmission (2DWPT) system. In our recent research, 2DWPT system has been improved in efficiency and electromagnetic compatibility (EMC), by covering the waveguide surface with a thick insulator layer and using a high-quality-factor (high- $Q$ ) resonant coupler. The rectifying coupler is a combination of a high- $Q$  waveguide-ring resonator (WRR) coupler and a class-F rectifying circuit. We evaluate the overall efficiency, i.e. the ratio of the dc output of the rectifying coupler to the RF input into the sheet, in a prototype 2DWPT system. A  $6.4 \times 3.6$  cm<sup>2</sup> coupler on a  $56 \times 39$  cm<sup>2</sup> sheet (nearly 100 times larger area than the coupler) achieved 40.4% efficiency at a maximum, where the RF input was 30.0 dBm in a 2.4-GHz band.

**Index Terms**—RF-dc converter, two-dimensional waveguide, waveguide-ring resonator, wireless power transmission.

## I. INTRODUCTION

A rectifying antenna (rectenna) is an essential component in wireless power transmission (WPT) systems using radio frequency (RF) electromagnetic waves (EM waves). It is an RF receiving antenna combined with a rectifying circuit, which converts RF power into dc power.

Microwave power transmission via the air is a convenient form of WPT. In the general environment, however, it is limited to low power density applications because of electromagnetic compatibility (EMC) problems. For example, the power density in the air is regulated by a guideline of human exposure to EM fields by The International Commission on Non-Ionizing Radiation Protection (ICNIRP) [1].

The authors have proposed two-dimensional waveguide power transmission (2DWPT), which has a potential to support higher-power WPT while the EM leakage conforms to the guideline [2], [3]. In 2DWPT systems, an EM wave propagates along a waveguide sheet and is received selectively by special receiver devices on the sheet.

2DWPT system also has an inevitable trade-off between the safety and the power transmission capacity. Our latest work [3] has demonstrated that EMC performance is improved by covering the waveguide surface with a thick insulator as shown in Fig. 1, and that a waveguide-ring resonator (WRR) coupler extracts significant power from the waveguide across the thick insulator. Extraneous objects near, or even touching, the sheet are not exposed to strong EM fields. The WRR coupler has a significantly high quality factor (high- $Q$ ) in the resonant state, which is essential to support such a selective power transmission.

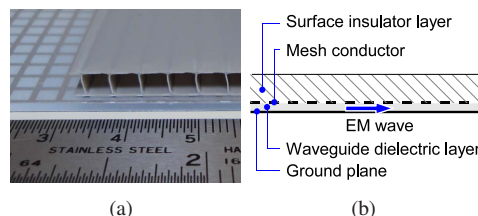


Fig. 1. (a) An upper view of a waveguide sheet around its edge and (b) a schematic drawing of its cross section.

In this paper, we examine the dc output efficiency of a rectifying coupler for the EMC-compliant 2DWPT. The term, rectifying coupler, is analogous to rectenna in over-the-air WPT. The high- $Q$  WRR coupler and a high-efficiency class-F RF-dc converter are integrated into the rectifying coupler. This paper presents a brief review of the WRR coupler and the class-F RF-dc converter circuit designed in our previous works, and reports measured characteristics of the integrated rectifying coupler. The dc output efficiency is defined as the ratio of the dc output power of the rectifying coupler to the RF input power fed into the waveguide sheet. The efficiency determines the maximum dc output under the condition where the RF power in the sheet is limited by the EMC guideline and is an essential evaluation factor. We demonstrate that the efficiency achieves 40.4% at a maximum, using a  $6.4 \times 3.6$  cm<sup>2</sup> rectifying coupler on a  $56 \times 39$  cm<sup>2</sup> sheet.

This paper is organized as follows. Section II and Section III present a brief review of the WRR coupler and the RF-dc converter, respectively. Section IV presents integrated rectifying coupler design and its characteristics measurement results. Finally, Section V concludes this paper.

## II. WAVEGUIDE-RING RESONATOR COUPLER

This section presents a brief review of a WRR, which is an RF coupling part of our rectifying coupler. The WRR is one of realizations of a high- $Q$  resonator, which is an essential element to improve the selectivity in 2DWPT systems [3].

As shown in Fig. 2, the WRR coupler and the waveguide sheet form together a flat waveguide-ring. Suppose that the thicknesses and the permittivities of the coupler dielectric and of the surface insulator layer are respectively equal to each other. The fundamental resonant mode appears at a frequency where the waveguide-ring perimeter become one wavelength.

The waveguide-ring is defected at the both ends of the coupler, i.e., the outer conductor of the waveguide is discon-

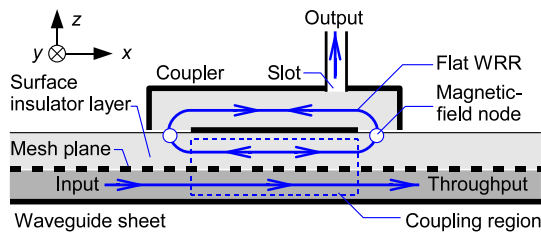


Fig. 2. A schematic drawing of a WRR coupler and a waveguide sheet. They form together a waveguide-ring whose perimeter is one wavelength. The thick lines represent conductors. Since the outer conductor of the waveguide-ring is discontinuous at the both ends of the coupler, the resonant mode has magnetic field nodes there.

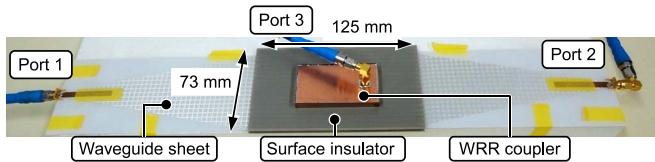


Fig. 3. Experimental setup to measure  $S$  parameters. The WRR coupler is put on a small ( $73 \times 125 \text{ mm}^2$ ) sheet.

tinuous there. It results in zero conduction current in the  $z$ -direction, which is equivalent to the zero magnetic field in the  $y$ -direction. In the resonant mode, the impedance at the both ends of the coupler is therefore significantly high, and the coupling between the resonant mode and the radiation mode is suppressed. Such a low radiation loss supports the high unloaded- $Q$  of the WRR coupler.

To couple to the resonant mode and to extract power, a slot coupling can be used. The slot is formed on the upper conductor wall of the WRR coupler and an output transmission line can be connected to the slot [3]. The impedance matching is performed by tuning the position and dimensions of the slot.

The evaluation setup of the fabricated WRR coupler is shown in Fig. 3. The waveguide sheet is the same as one designed in [3]. The both ends of the 73-mm wide sheet are connected to 50- $\Omega$  coaxial lines via horn-like impedance matching patterns of the sheet and standing wave in the sheet is eliminated. One of the ends is referred to as port 1 (input port), the other is referred to as port 2 (absorption port). The output port of the coupler on the sheet is port 3.

The measured scattering parameters ( $S$  parameters) are shown in Fig. 4. The peak value of  $|S_{31}|$  is  $-5.77 \text{ dB}$ , which means that 26.5% of the power fed into the sheet is extracted as the coupler RF output. The coupler output impedance is well matched to 50  $\Omega$  and  $|S_{33}| = -21.0 \text{ dB}$  at the same frequency.

### III. CLASS-F RF-DC CONVERTER

This section presents a brief description of our class-F RF-dc converter circuit. RF-dc converter circuits including the source and the load typically consist of five elements: 1) the RF source, 2) an input filter, 3) one or several number of diodes, 4) an output filter, and 5) the dc load.

In the frequency domain, the diodes generate harmonics, and the filters therefore have to reject power dissipation

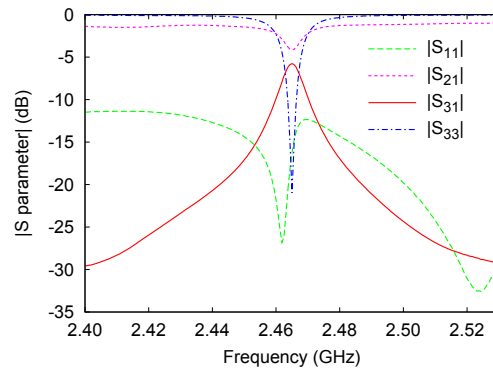


Fig. 4. Measured  $S$  parameters. The peak  $|S_{31}|$  is  $-5.77 \text{ dB}$  at 2.465 GHz.

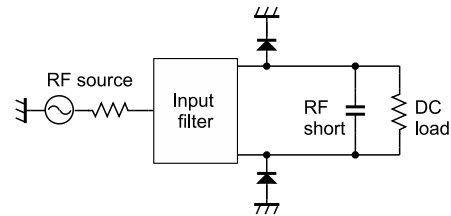


Fig. 5. Antisymmetric RF-dc converter circuit that realizes class-F operation. Two parallelized single-shunt rectifying circuits form a horizontally symmetric structure, except the diode polarities opposite to each other. They are driven by a common-mode RF signal and the dc output appears as a differential-mode, across the resistor. The RF-short capacitor eliminates the differential-mode even harmonic voltages across itself. The input filter is needed for common-mode odd harmonic currents rejection.

by those harmonics to improve the conversion efficiency. A fundamental requirement for the filters to reduce harmonics power dissipation is to have a reflection coefficient nearly equal to 1 (ideally equal to 1 but actually less than 1) at every harmonic frequency. Additionally, the efficiency also depends on the arguments of the complex reflection coefficients, which affect the waveforms of voltage and current across the diodes and determine the maximum power handling capacity while not damaging or breaking down the diodes.

For practical Schottky barrier RF diodes having a low breakdown voltage and a relatively large on-state resistance, class-F operation is efficient [4], [5]. In the ideal class-F operation, even-harmonic voltages and odd-harmonic currents across the diodes are rejected and the harmonic power dissipations are eliminated.

The antisymmetric circuit configuration proposed in our previous work [6] is shown in Fig. 5. In this configuration, only odd harmonics current rejection filter at the input-side is needed to realize class-F operation. The simplest realization where only a third harmonic rejection filter is implemented is designed as shown in Fig. 6.

The voltage and current spectra across diode  $D_1$  are calculated through EM/circuit co-simulations and harmonic balance simulations using CST Studio Suite and are shown in Fig. 7. The result shows that the second and the fourth harmonic voltages and the third harmonic current are relatively small and the rectifier realizes an approximate class-F operation.

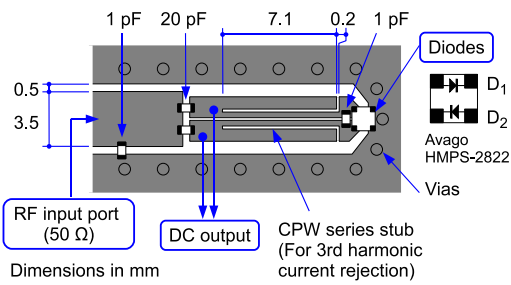


Fig. 6. RF-dc converter circuit. The pattern is formed on one side of a 1.524-mm thick double-sided copper clad board, Arlon DiClad-880. Input microwave is fed from the 50-Ω coplanar waveguide (CPW) on the left hand side and conducted to the next 60-Ω CPW through the 20-pF capacitors. The 60-Ω CPW live conductor is split at the center by a 0.2-mm thick slot for dc isolation. Inside the 60-Ω CPW, another smaller 60-Ω CPW is formed by two L-shaped 0.2-mm thick slots. The smaller CPW becomes quarter-wavelength and rejects the current at the third harmonic frequency.

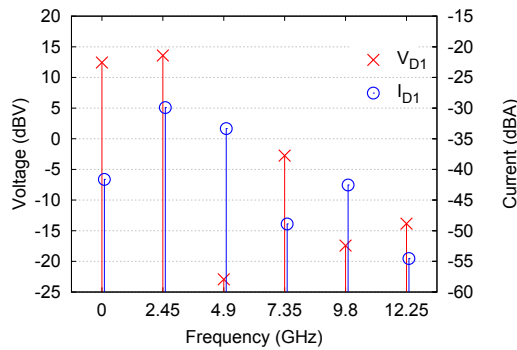


Fig. 7. Spectra of the simulated voltage and current across the diode  $D_1$ . The reference values are 0 dBV = 1 V and 0 dBA = 1 A.

A fabricated circuit was evaluated with a measurement setup shown in Fig. 8. The incident RF power  $P_{in}$  is measured by the power meter, Agilent E4418B, through the directional coupler. The fundamental frequency component of the reflected power,  $P_{ref}$ , is measured by the spectrum analyzer, Agilent N9342C. The output voltage  $V_{out}$  across the load resistor  $R_L$  is measured by the voltmeter, and the power consumption  $P_{out}$  at the load is calculated as  $P_{out} = V_{out}^2/R_L$ .

The incident power dependence of the RF-dc conversion efficiency  $P_{out}/P_{in}$  and the reflection coefficient  $P_{ref}/P_{in}$  are shown in Fig. 9, where the frequency is fixed at 2.45 GHz. The maximum efficiency is 77.9% at  $P_{in} = 27$  dBm and the efficiency fluctuation depending on the frequency is less than 0.5% throughout a 2.4–2.5 GHz band, where  $P_{in} = 20.0$  dBm.

#### IV. INTEGRATED RECTIFYING COUPLER

In this section we evaluate a rectifying coupler, into which the WRR coupler and the RF-dc converter presented in the previous sections are integrated. The top view of a designed rectifying coupler is shown in Fig. 10 and a fabricated one is shown in Fig. 11.

The rectifying coupler was evaluated in a setup shown in Fig. 12. The sheet is the same as one used in Section II, and the rectifying coupler is placed on it, similarly to Fig. 3. The incident power into the input port,  $P_{in}$ , is measured by the

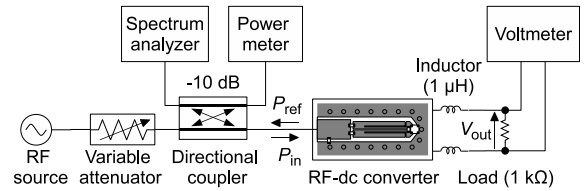


Fig. 8. RF-dc conversion efficiency measurement setup. The frequency and the power of the microwave fed into the circuit are swept and corresponding dc outputs are measured.

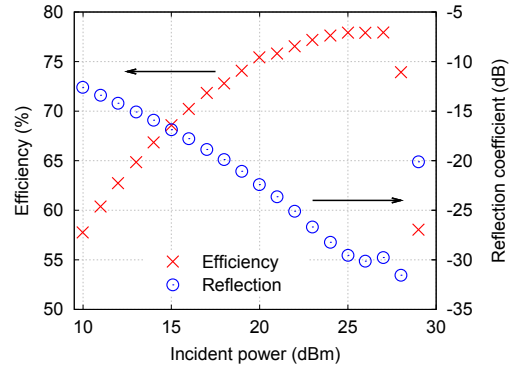


Fig. 9. Measured conversion efficiency and reflection coefficient versus the incident power. The input RF frequency is fixed at 2.45 GHz. The peak efficiency is 77.9% at  $P_{in} = 27$  dBm. The steep efficiency drop above 28 dBm is due to the breakdown of the diodes.

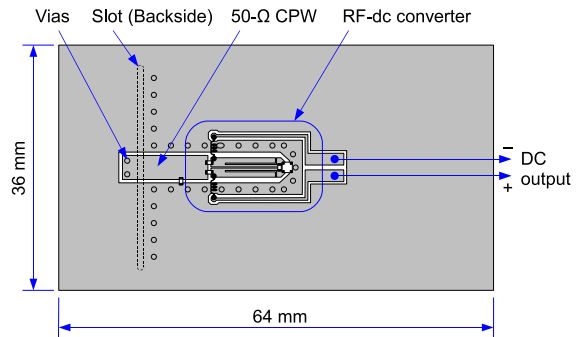


Fig. 10. The top board of the rectifying coupler. The RF-dc converter is formed on the top side of a 1.524-mm thick double-sided copper clad board, the same one as shown in Fig. 6. A slot is formed on the bottom side. The 50-Ω-matched slot and the 50-Ω CPW are connected by vias.

power meter. The reflected power at the port,  $P_{ref}$ , and the transmitted power to the absorption port,  $P_{thru}$ , are measured by the spectrum analyzer one by one. The coupler dc output power  $P_{out}$  is calculated from the measured dc output voltage across the 1-kΩ load resistor.

The dc output efficiency is defined as  $P_{out}/P_{in}$ . The EMC requirement on the RF emission determines the maximum acceptable RF power in the sheet. The dc output power under this limitation on the RF power is an essential evaluation factor, and the ratio of the coupler dc output power to the sheet RF input power is a reasonable definition of the efficiency.

The frequency dependence is shown in Fig. 13.  $P_{in}$  was fixed at 30.0 dBm. All the results are plotted in dB, where the

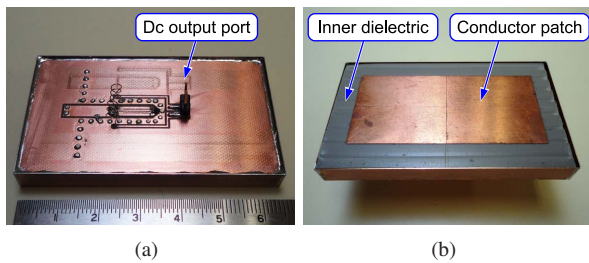


Fig. 11. (a) An upper view and (b) an under view of a fabricated rectifying coupler.

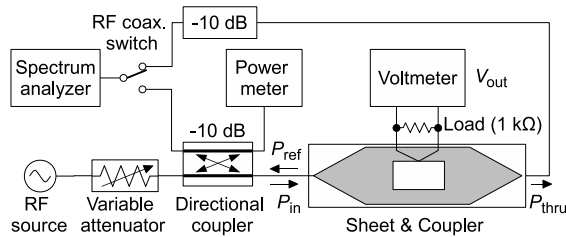


Fig. 12. Evaluation setup of the fabricated rectifying coupler. The sheet is the same as one used in Fig. 3. The unselected port of the RF switch is terminated with  $50\text{-}\Omega$ .

incident power is used as the reference value (0 dB). The peak dc output, 19.0% ( $-7.21$  dB) of the incident power, appears at 2.465 GHz.

From Fig. 4, the coupler RF output is estimated to be approximately 24.2 dBm ( $\approx 30.0$  dBm  $- 5.77$  dB). From this estimation and Fig. 9, the dc output of the RF-dc converter is predicted to be approximately 203 mW ( $\approx 24.2$  dBm  $\times 77.2\%$ ), which well agrees with the measured result (190 mW). Thus, both of the WRR coupler and the RF-dc converter work well in the integrated form.

Finally, we measured the coupler output on a large sheet as shown in Fig. 14. The coupler output depends on its position on the sheet. The coupler was moved around on the sheet and the output was measured. The highest dc output efficiency found in our trial-and-error was 40.4%, while the input was 30.0 dBm. Based on a rough evaluation, efficiency maxima around 20-30% appear periodically with approximately a half-wavelength period ( $\approx 5$  cm).

The highest efficiency is approximately twice as high as the peak efficiency in Fig. 13. This is due to the symmetric directivity of the coupler and to existence of a standing wave in the open-edged sheet. In Fig. 14, the coupler is excited by the incident (rightward) wave and by the reflected (leftward) wave, which is suppressed in Fig. 12. The output therefore become twice at anti-node positions of the magnetic field.

## V. CONCLUSION

High-efficiency dc power extraction from a 2-D waveguide by a rectifying coupler was demonstrated. Both the WRR coupler and the RF-dc converter worked well in the integrated form. The dc output efficiency achieved 40.4% at a maximum, using a  $6.4 \times 3.6$  cm<sup>2</sup> rectifying coupler on a  $56 \times 39$  cm<sup>2</sup> sheet, which had nearly 100 times larger area than the coupler.

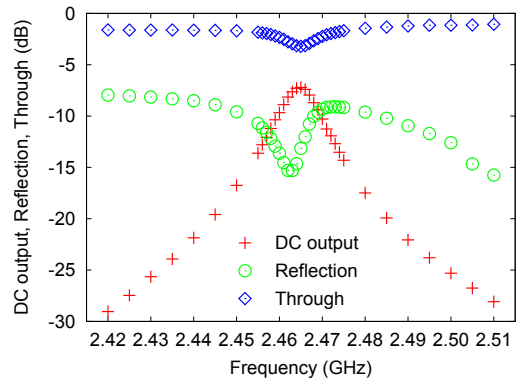


Fig. 13. Measured characteristics of the system shown in Fig. 12.

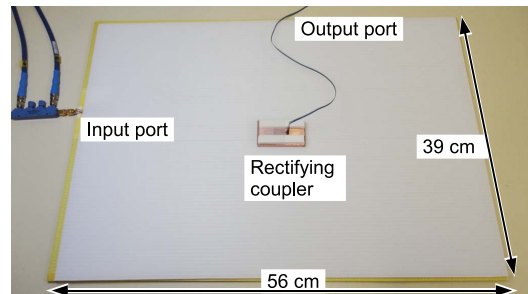


Fig. 14. Rectifying coupler evaluation on a large sheet. The sheet edges are open and cause EM wave reflections. The coupler output efficiency achieved 40.4% at a maximum, where the input was 30.0 dBm.

Since the efficiency maxima around 30% appear periodically, the transmission efficiency can achieve 30% for arbitrary receiver position by controlling the standing wave in the sheet. By using multiple feeding points on a sheet edge and tuning their phases, the standing wave can be controlled. Developing such a tunable multi-input 2DWPT system is a future work.

## ACKNOWLEDGMENT

The research was partly supported by National Institute of Information and Communications Technology (NICT) 13701 and by Grant-in-Aid for JSPS Fellows (22-6659).

## REFERENCES

- [1] International Commission on Non-Ionizing Radiation Protection, "Guidelines for limiting exposure to time-varying electric, magnetic, and electromagnetic fields (up to 300 GHz)," *Health Physics*, vol. 74, no. 4, pp. 494-522, 1998.
- [2] H. Shinoda, Y. Makino, N. Yamahira, and H. Itai, "Surface sensor network using inductive signal transmission layer," in *Proc. INSS 2007*, 2007, pp. 201-206.
- [3] A. Noda and H. Shinoda, "Selective wireless power transmission through high-Q flat waveguide-ring resonator on 2-D waveguide sheet," *IEEE Trans. Microw. Theory Tech.*, vol. 59, no. 8, pp. 2158-2167, 2011.
- [4] J. A. Hagerty, "Nonlinear circuits and antennas for microwave energy conversion," Ph.D. dissertation, University of Colorado, 2003.
- [5] K. Hatano, N. Shinohara, T. Mitani, K. Nishikawa, T. Seki, and K. Hiraga, "Development of class-F load rectennas," in *Proc. IMWS-IWPT 2011*, 2011, pp. 251-254.
- [6] A. Noda and H. Shinoda, "Compact class-F RF-dc converter with anti-symmetric dual-diode configuration," in *IMS 2012 Digest*, to be published in June 2012.